

accounts for the short U-C(1) and P-C(1) bonds. While this model necessarily would be altered if there is additional bonding between the $[\text{Cp}_3\text{U}]^+$ and $[\text{CHPR}_3]^-$ groups, the neutron data, which indicate a normal $\alpha\text{-C}(1)\text{H}(1)$ group, support the bonding description summarized above. The closest intramolecular nonbonding contacts are 2.13 Å, H(1)···H(13), and 2.21 Å, H(3B)···H(24) (Figure 2). Both are considerably less than 2.4 Å, twice the van der Waals radius for hydrogen, and suggests that $\text{Cp}_3\text{U}=\text{CHPR}_3$ is sterically crowded. These contacts thus may indicate that the large U-C-P angle is not due to electronic effects alone but rather also reflects repulsion between PMe_3 and Cp groups; Figure 2 illustrates the crowding effect.

Within the CHPR_3 moiety bond angles and distances are normal, and as in other $\text{Cp}_3\text{U-X}$ type molecules, the geometry about uranium is roughly tetrahedral.⁴ The average U-C(Cp) distance of 2.8 Å is normal for U^{IV} systems.² Due to the high precision of the neutron results, the small differences in individual U-C(Cp) distances (2.764 (1)–2.819 (1) Å) are statistically significant. A projection down the U-C(1) axis is shown in Figure 2 where only those U-C(Cp) distances that are less than the average U-C(Cp) distance for each Cp group are represented as bonds. In each case, one side of the Cp ring lies closer

to the uranium than the other, so that the Cp planes are not perpendicular to the vector joining the uranium with their respective centroids (88.7° for Cp(1), 88.5° for Cp(2), and 89.1° for Cp(3)). The closest intramolecular contacts between the hydrogens on neighboring Cp groups, Table IV, are near or somewhat less than 2.4 Å. Thus, the slight, screwlike canting of the Cp groups is probably a steric effect.

Acknowledgment. The support of this work by the National Science Foundation, Grants CHE 85-12989 (J. W.G. and R.E.C.) and CHE 87-03425 (R.B.), the donors of the Petroleum Research Fund, administered by the American Chemical Society (R.E.C. and J.W.G.), and the W. C. Hamilton Memorial Scholarship (R.C.S.) is gratefully acknowledged. Work at Brookhaven National Laboratory was performed under Contract DE-AC02-76CH00016 with the U.S. Department of Energy, Office of Basic Energy Sciences (T.F.K.). The technical assistance of J. Guthy and D. Rathjen during the neutron diffraction experiment is gratefully appreciated. Finally, we thank L. Brammer for his careful review of the manuscript and helpful suggestions for its improvement.

Supplementary Material Available: Tables S1 (anisotropic temperature factors) and S2 (bond distances (Å) and angles (deg)) (4 pages); Table S3 (observed and calculated squared structure factors) (43 pages). Ordering information is given on any current masthead page.

EPR Spectrum of the $\text{Fe}_2(\text{CO})_8^-$ Radical Trapped in Single Crystals of $\text{PPN}^+\text{HFe}_2(\text{CO})_8^-$

Paul J. Krusic

Central Research and Development Department, E. I. du Pont de Nemours and Company, Wilmington, Delaware 19898

John R. Morton, Keith F. Preston,* Antony J. Williams, and Florence L. Lee

Division of Chemistry, National Research Council of Canada, Ottawa, Ontario, Canada K1A 0R9

Received August 2, 1989

Solid $\text{PPN}^+\text{HFe}_2(\text{CO})_8^-$ prepared by literature methods exhibits an intense EPR spectrum due to the presence of a paramagnetic impurity. Comparison with the spectrum in frozen solutions of $\text{Na}^+\text{Fe}_2(\text{CO})_8^-$ in 2-MeTHF shows that the signal is due to the $\text{Fe}_2(\text{CO})_8^-$ radical. The EPR signal in single crystals of the material is anisotropic and obeys the symmetry operations of the lattice space group ($P2_1/c$). Measurements made with crystallographically aligned specimens show that, within experimental error, the principal directions of the \mathbf{g} -tensor (principal values 2.0093, 2.0538, 2.0579) are determined by the local symmetry (C_{2v}) of the host anion. It is concluded that the $\text{Fe}_2(\text{CO})_8^-$ radical retains the symmetry of the host anion and thus has two bridging carbonyl ligands. The orientation of the components of \mathbf{g} and their displacement from the free-spin value conform with the results of extended Hückel calculations, which place the unpaired electron in a b_2 orbital that is antibonding in the Fe-Fe distance.

Introduction

The variety of modes available to carbon monoxide in bonding to transition-metal atoms¹ results in a wealth of structures among the metal carbonyls and raises many possibilities for isomerism. Energy differences between isomers, such as bridged and unbridged versions of the same molecule, are often small, so that subtle changes in environment may sometimes favor one structure over an-

other. $\text{Co}_2(\text{CO})_8$, for example, exists as a doubly bridged form in the pure solid² and as unbridged forms in solution and frozen matrices.³⁻⁶ An even more striking example

(1) Cotton, F. A.; Wilkinson, G. *Advanced Inorganic Chemistry*, 5th ed.; Wiley: New York, 1988; Chapter 22.

(2) Sumner, G. F.; Klug, H. P.; Alexander, L. E. *Acta Crystallogr.* 1964, 17, 732.

(3) Bor, G.; Noack, K. *J. Organomet. Chem.* 1974, 64, 367.

(4) Bor, G.; Dietter, U. K.; Noack, K. *J. Chem. Soc., Chem. Commun.* 1976, 914.

(5) Sweaney, R. L.; Brown, T. L. *Inorg. Chem.* 1977, 16, 415.

* NRCC No. 31043, Du Pont Contribution No. 5305.

is provided by the isoelectronic series $\text{Co}_2(\text{CO})_8$, $\text{FeCo}(\text{C}-\text{O})_8^-$, and $\text{Fe}_2(\text{CO})_8^{2-}$, whose members have structures in the solid state containing two, one, and no carbonyl bridges, respectively.⁷ This type of isomerism has also been established⁸⁻¹⁴ for coordinatively unsaturated and odd-electron metal carbonyls. Our recent EPR studies¹⁴ of doped single crystals of $\text{PPN}^+\text{FeCo}(\text{CO})_8^-$, for example, demonstrate that the $\text{Fe}_2(\text{CO})_8^-$ radical is present in that host in two isomeric forms that are in thermal equilibrium. One of these isomers clearly had the singly bridged asymmetric structure of the host; it was surmised that the other, less stable isomer possessed two carbonyl bridges and C_{2v} symmetry. Spectroscopic evidence obtained from liquid and frozen solutions of $\text{Fe}_2(\text{CO})_8^-$ support the proposed structure for the latter isomer^{14,15} but indicate that it is the more stable form in the "free state". To confirm the structure of this form of the radical, we sought to dope it into an appropriate single-crystal host. EPR measurements of polycrystalline samples of the compound¹⁶ $\text{PPN}^+\text{HF}_2(\text{CO})_8^-$ show that it contains that particular form of the $\text{Fe}_2(\text{CO})_8^-$ radical as an adventitious impurity. In this article we report our EPR measurements on single crystals of that material and the inferences drawn therefrom.

Experimental Section

The compound $\text{PPN}^+\text{HF}_2(\text{CO})_8^-$ was prepared by the method of Hieber and Brendel¹⁷ following the detailed experimental procedure used in the X-ray crystallographic structural determination.¹⁶ The largest crystals, which had a maximum dimension of ≈ 1 mm, were removed from the product and examined under a polarizing microscope. Single crystals were selected and oriented on a Picker diffractometer according to the known structural parameters.¹⁶ Once oriented, the crystals were sealed with epoxy glue into the ends of 4-mm quartz tubes such that each of the standard set¹⁸ of orthogonal axes X, Y, Z in turn was aligned along the tube axis. The direction of a second axis in the plane perpendicular to the tube was indicated by a pointer glued to the tube.

Each tube containing its embedded single crystal was suspended vertically in a Dewar of liquid nitrogen such that the crystal was positioned at the center of a resonant rectangular microwave cavity. The tube pointer, which corresponded to a crystal axis, then lay immediately above a horizontal brass protractor marked every 5° of arc. Rotating the tube about its axis caused the dc magnetic field to explore a plane of this crystal. EPR spectra were recorded at regular angular intervals throughout each crystal plane on a Varian E12 spectrometer equipped with standard accessories for the measurement of microwave frequency and magnetic-field intensity. A spectrum was also recorded and measured for a crystal aligned so that B_0 lay along the direction (1,1,1) in the orthogonal crystal axis system.

Results

For a random orientation of the dc magnetic field, the

- (6) Onaka, S.; Shriver, D. F. *Inorg. Chem.* **1976**, *15*, 915.
 (7) Chin, H. B.; Smith, M. B.; Wilson, R. D.; Bau, R. *J. Am. Chem. Soc.* **1974**, *96*, 5285.
 (8) Poliakoff, M.; Turner, J. J. *J. Chem. Soc. A* **1971**, 2403.
 (9) Sweany, R. L.; Brown, T. L. *Inorg. Chem.* **1977**, *16*, 415.
 (10) Hepp, A. F.; Wrighton, M. S. *J. Am. Chem. Soc.* **1983**, *105*, 5934.
 (11) Krusic, P. J.; San Filippo, J., Jr.; Hutchinson, B.; Hance, R. L.; Daniels, L. M. *J. Am. Chem. Soc.* **1981**, *103*, 2129.
 (12) Lionel, T.; Morton, J. R.; Preston, K. F. *Inorg. Chem.* **1983**, *22*, 145.
 (13) Baker, R. T.; Krusic, P. J.; Calabrese, J. C.; Roe, D. C. *Organometallics*, **1986**, *5*, 1506.
 (14) Morton, J. R.; Preston, K. F.; Le Page, Y.; Krusic, P. J. *J. Chem. Soc., Faraday Trans. 1* **1989**, *85*, 4019.
 (15) Krusic, P. J.; Subra, R. *J. Am. Chem. Soc.*, in press.
 (16) Chin, H. B.; Bau, R. *Inorg. Chem.* **1978**, *17*, 2314.
 (17) Hieber, W.; Brendel, G. *Z. Anorg. Allg. Chem.* **1957**, *289*, 324.
 (18) Rollett, J. S. *Computing Methods in Crystallography*; Pergamon: London, 1965; Chapter 3.

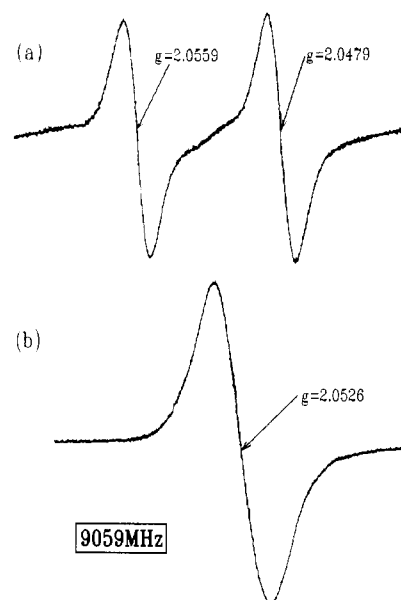


Figure 1. First-derivative EPR spectra at 77 K for a single crystal of $\text{PPN}^+\text{HF}_2(\text{CO})_8^-$ for (a) B_0 10° from Y in YZ and (b) $B_0 \parallel Y$.

Table I. g^2 Tensor for $\text{Fe}_2(\text{CO})_8^-$ in a Single Crystal of $\text{PPN}^+\text{HF}_2(\text{CO})_8^-$ Together with the Principal Values of g and Their Directions in the XYZ Axis System

g^2 tensor			principal values and direction cosines of g		
$X(a^*)$	$Y(b)$	$Z(c)$	xx	yy	zz
			2.0579	2.0538	2.0093
4.1583	± 0.0405	0.0772	0.3278	0.7426	-0.5840
± 0.0405	4.2126	∓ 0.0472	± 0.9308	∓ 0.1479	± 0.3344
0.0772	∓ 0.0472	4.1197	-0.1620	0.6532	0.7397

EPR spectrum of a single crystal of $\text{PPN}^+\text{HF}_2(\text{CO})_8^-$ at 77 K consisted of two absorptions (Figure 1) of equal intensity with a peak-to-peak line width of ≈ 2 G. Due to the exceptionally small size of the crystals the signal was quite weak, and satellite absorptions attributable to ^{13}C or ^{57}Fe were not detected under any conditions. Along the $X(a^*)$, $Y(b)$, and $Z(c)$ axes and throughout the XZ plane the spectrum consisted of a single resonance; for off-axis directions in XY and YZ this single line split into two. This behavior is typical of "site splitting" in a monoclinic crystal.¹⁹ The spectrum did not change significantly in the temperature range 4–140 K. Above 140 K, the line width increased with increasing temperature, and the signal was not detectable at temperatures in excess of 290 K.

g^2 values for the two sites varied sinusoidally, as expected,¹⁹ with angular displacement in each of the crystal planes (Figure 2). A linear regression computer routine¹⁹ was used to obtain the diagonal and off-diagonal g^2 matrix elements (Table I) that best fit (Figure 2) the experimental data. Uncertainty in the relative signs of the off-diagonal elements for XY and YZ was resolved by comparing the measured g values for $B_0/(1,1,1)$ with those calculated for the two possible sign choices.¹⁹ Computerized diagonalization led to the principal values of g and their directions in the XYZ crystal-axis system (Table I).

Discussion

In considering the identity of the carrier in $\text{PPN}^+\text{HF}_2(\text{CO})_8^-$, we note that its principal g values correspond closely to those for^{14,15} the persistent radical $\text{Fe}_2(\text{CO})_8^-$ when doped as the sodium salt into 2-MeTHF (2.0091,

(19) Morton, J. R.; Preston, K. F. *J. Magn. Reson.* **1983**, *52*, 457.

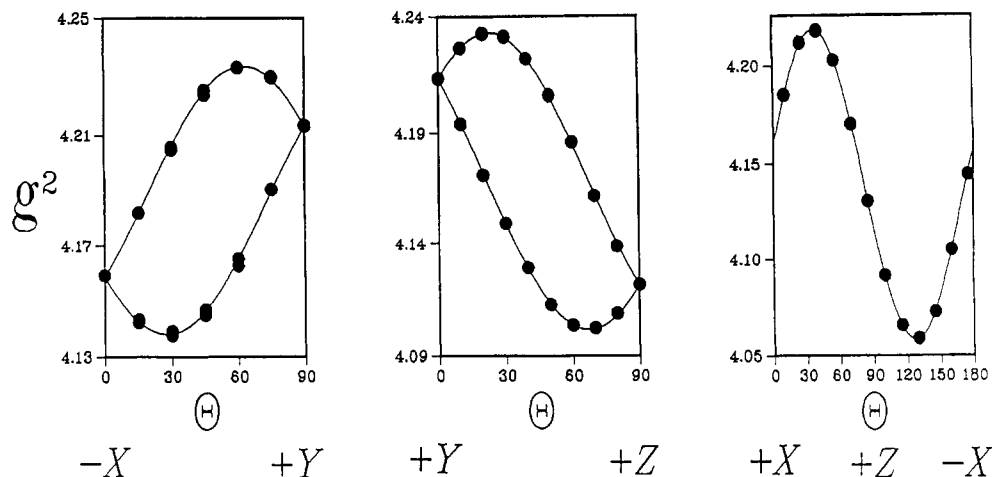


Figure 2. g^2 values as a function of angle in the three orthogonal crystal planes.

Table II. Certain Unit Vectors within the Anion of the $PPN^+HFe_2(CO)_8^-$ Crystal

direction	direction cosines			angle to g
	X	Y	Z	
H to bisector of C_7, C_8 perpendicular to Fe_1-H-Fe_2 plane	-0.6625	± 0.3697	0.6514	7° to g_{min}
Fe_1-H-Fe_2 plane	0.1824	± 0.9243	-0.3352	13° to g_{max}
C_7-H-C_8 plane	0.7278	± 0.1124	0.6765	15° to g_{int}

2.0501, 2.0555). The same species was undoubtedly also observed in liquid and frozen THF as a product of the reduction of $Fe(CO)_5$ by sodium.¹¹ (In THF, however, the greater spectral line width obscured the slight nonaxiality in the g tensor, and the powder spectrum was analyzed in terms of $g_{||} = 2.0092$, $g_{\perp} = 2.0540$.) Furthermore, a very similar set of principal g values (2.0092, 2.0537, 2.0619) was assigned¹⁴ to one of two isomers of $Fe_2(CO)_8^-$ observed in $PPN^+FeCo(CO)_8^-$ single crystals doped with $PPN^+Fe_2(CO)_8^-$. There can be little doubt, therefore, that the free radical naturally present in $PPN^+HFe_2(CO)_8^-$ is $Fe_2(CO)_8^-$; its structure, however, still remains to be determined.

The pattern of behavior established for the two magnetically inequivalent sites (Figure 2) is characteristic of a monoclinic crystal and shows that the impurity $Fe_2(CO)_8^-$ radical obeys the space group symmetry¹⁶ ($P2_1/c$) of the host. This in turn strongly suggests that the radical substitutes for the host anion in the crystal structure. Accordingly, we now attempt to relate the principal directions of g to directions within the host anion.

In attempting to find a correlation between the principal directions of g and directions within the host crystal structure, it is important to take into consideration the near-axial nature of the tensor for $Fe_2(CO)_8^-$. In this situation the eigenvector associated with the unique g value (g_{min}) is well defined, whereas the eigenvectors associated with the two nearly equal principal values are poorly defined. Correlations with g_{min} will clearly, therefore, be more significant than with the other components of the tensor. To a very good approximation the host cation $HFe_2(CO)_8^-$ has C_{2v} symmetry¹⁶ (Figure 3) in which the planes defined by Fe_1-H-Fe_2 and by C_7-H-C_8 are near mirror planes and the line joining H to the bisector of C_7 and C_8 is a 2-fold axis (z). The unit vectors in the XYZ basis for this 2-fold axis and for the perpendiculars to the two symmetry planes are given in Table II. We see that g_{min} lies only 7° from the 2-fold axis, g_{int} lies 15° from the perpendicular to C_7-H-C_8 , and g_{max} lies 13° from the perpendicular to Fe_1-H-Fe_2 . In view of the estimated error of $\approx 5^\circ$ in the transfer of crystals from the X-ray diffractometer and the poor definition of the eigenvectors associated with g_{int} and

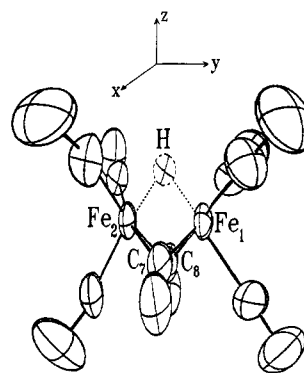


Figure 3. Structure of the $HFe_2(CO)_8^-$ anion in $PPN^+HFe_2(CO)_8^-$ as proposed in ref 16. Dashed lines indicate loss of H atom to give the proposed structure of the $Fe_2(CO)_8^-$ impurity centre.

g_{max} , we can justifiably claim to have established a close correlation between the principal directions of g and the symmetry elements of the host anion: the $Fe_2(CO)_8^-$ radical has evidently adopted the symmetry of the $HFe_2(CO)_8^-$ anion and thus has two bridging carbonyl ligands (Figure 3).

The $Fe_2(CO)_8^-$ radical has now been identified in two distinct isomeric forms in two different single-crystal hosts, $PPN^+HFe_2(CO)_8^-$ and $PPN^+FeCo(CO)_8^-$. In both cases, the free radical adopts the geometry of the host anion as its most stable structure within the solid. It would appear that the host determines the geometry of the guest when it is a substitutional impurity, and the structure of $Fe_2(CO)_8^-$ in the "free state" remains a moot point. However, the available experimental evidence points to the doubly bridged C_{2v} form as the more stable of the two isomers: First and most importantly, we note that g components appropriate to the C_{2v} form were measured^{11,15} in frozen THF and 2-MeTHF. Furthermore, the isotropic g value measured in the liquid solvents^{11,15} (2.0385) corresponds much better with one-third of the trace of g for the doubly bridged form (2.0405) than with $Tr |g|/3$ the other isomer¹⁴ (2.0535). Second, we recall that the isotropic spectrum shows hyperfine coupling to two equivalent ^{57}Fe nuclei in samples appropriately enriched in the magnetic isotope of iron.¹¹ Of the two isomers, only the C_{2v} form contains geometrically equivalent iron nuclei; the low-symmetry form (C_s) has the unpaired spin density essentially confined to one iron nucleus.¹⁴ Admittedly, this particular argument is weakened by the likely occurrence of rapid fluxional processes at elevated temperatures that could render the two Fe nuclei in the C_s isomer equivalent on the EPR time scale. Last, we note that only one isomer

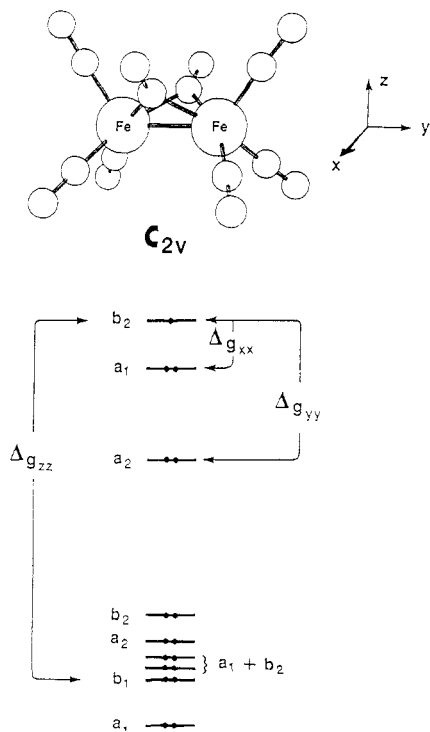


Figure 4. Upper filled levels of $\text{Fe}_2(\text{CO})_8^-$ in C_{2v} geometry from extended Hückel calculations and symmetry-allowed g shifts. The levels are drawn roughly to scale from the calculated energies.

of $\text{Fe}_2(\text{CO})_8^-$ is observed from 4 to 150 K in $\text{PPN}^+\text{HFe}_2(\text{CO})_8^-$, whereas both are observed¹⁴ in $\text{PPN}^+\text{FeCo}(\text{CO})_8^-$ in the range 4–70 K. Although the C_s isomer was the more stable in the latter host, the C_{2v} isomer persisted at low temperatures, giving rise to a distinctly curved van't Hoff plot.¹⁴ This again is an indication that the doubly bridged isomer is the energetically preferred form in the free state.

Thorn and Hoffman²⁰ have reported the results of a molecular orbital study of the $\text{Fe}_2(\text{CO})_8^{2-}$ anion in both bridged and unbridged C_{2v} geometries. For the doubly bridged species, they predict a b_2 HOMO that is remote from empty orbitals but close to a number of filled orbitals, all of which have substantial Fe 3d character. Upon removal of one electron from the b_2 orbital to give a 2B_2 ground-state free radical, it is possible to show that the orbital scheme of Thorn and Hoffman is completely consistent with the measured principal values of g for $\text{Fe}_2(\text{C}-\text{O})_8^-$. We have, in fact, repeated the calculations of Thorn and Hoffman²⁰ for a radical geometry identical with that¹⁶ of the undamaged hydridocarbonyl anion after removal of the hydrogen atom. Using the du Pont implementation of the extended Hückel method^{21,22} and the parameters of Thorn and Hoffmann²⁰ rather than those of McKinney et al.,²² our calculations (Figures 4 and 5) agree closely with those made earlier.²⁰ First, we note that the remoteness of the empty levels ensures that all of the g components

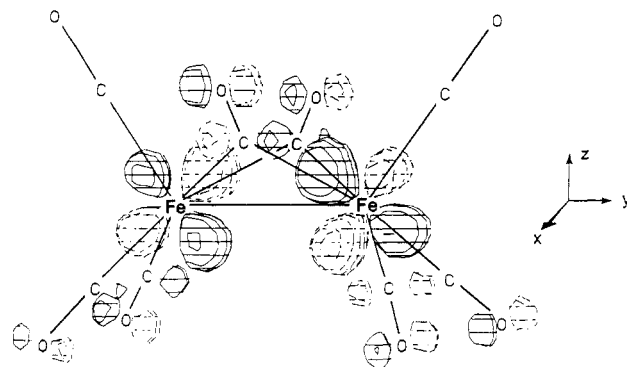


Figure 5. b_2 SOMO of C_{2v} isomer of $\text{Fe}_2(\text{CO})_8^-$ suggested by extended Hückel calculations made for the radical using the known geometry of $\text{HFe}_2(\text{CO})_8^-$ in $\text{PPN}^+\text{HFe}_2(\text{CO})_8^-$.

will be greater than the free-spin value (2.0023). Second, the direct products of R_x , R_y , and R_z with B_2 in C_{2v} are A_1 , A_2 , and B_1 , respectively. Thus, the predicted g shifts decrease in the observed order $\Delta g_{xx} > \Delta g_{yy} > \Delta g_{zz}$, because the relative energies of the filled orbitals in the extended Hückel scheme (Figure 4) are $E(a_1) > E(a_2) > E(b_1)$. (The b_1 orbital is one of a cluster of six closely spaced orbitals, all of which were not shown in the original article of Thorn and Hoffman.) Our extended Hückel calculations for $\text{Fe}_2(\text{CO})_8^-$ predict a b_2 SOMO with the atomic orbital composition shown in Figure 5. The SOMO has substantial contributions from both Fe 3d orbitals and smaller contributions from six C and six O atomic 2p_y orbitals. Unfortunately, the only experimental nuclear hyperfine interaction available for comparison with our theoretical predictions of unpaired spin density in $\text{Fe}_2(\text{CO})_8^-$ is the isotropic value of 3.7 G for the two equivalent ⁵⁷Fe nuclei.¹¹ This compares very favorably with the usual core-polarization term of (–)10 G for a single Fe 3d electron.²³

The evidence adduced here and elsewhere^{11,14,15} strongly supports a doubly bridged C_{2v} structure for the ground state of the $\text{Fe}_2(\text{CO})_8^-$ radical. A singly bridged C_s version has also been observed¹⁴ in a matrix that apparently “imposed” its structure on the guest radical. Yet a third isomer, without carbonyl bridges, is anticipated by the D_{3d} structures observed for ${}^7\text{Fe}_2(\text{CO})_8^{2-}$ in $(\text{PPN}^+)_2\text{Fe}_2(\text{CO})_8^{2-}$, for matrix-isolated^{3–6} $\text{Co}_2(\text{CO})_8$, and for matrix-isolated⁸ $\text{Fe}_2(\text{CO})_8$. The obvious host for such an isomer of the $\text{Fe}_2(\text{CO})_8^-$ radical is the known crystalline material⁷ $(\text{PPN}^+)_2\text{Fe}_2(\text{CO})_8^{2-}$, yet our attempts to generate a spectrum of the radical in that matrix have failed thus far. In the case of the neutral $\text{Fe}_2(\text{CO})_8$ carbonyl, infrared spectroscopic evidence suggests that the D_{3d} unbridged form is the most stable isomer⁸. This is evidently not the case for the free radical anion. Quite apart from the ESR evidence, the infrared spectrum of the radical in solution clearly shows the presence of bridging carbonyls.¹⁵

Acknowledgment. We are indebted to Dr. D. L. Thorn for helpful discussion and to R. Dutrisac and S. A. Hill for technical assistance.

(20) Thorn, D. L.; Hoffman, R. *Inorg. Chem.*, **1978**, *17*, 126.

(21) Anderson, A. B. *J. Chem. Phys.* **1975**, *62*, 1187. Anderson, A. B. *J. Am. Chem. Soc.* **1978**, *100*, 1153.

(22) Pensak, D. A.; McKinney, R. J. *Inorg. Chem.* **1979**, *18*, 3407. McKinney, R. J.; Pensak, D. A. *Ibid.* **1979**, *18*, 3413.

(23) Symons, M. C. R. *Chemical and Biochemical Aspects of Electron-Spin Resonance Spectroscopy*; Wiley, New York, 1978; Chapter 12.